3. Finite Element Analysis of Shear Behavior of RC Members with High Strength Materials

-Panels, Shear Walls, Beams, Columns and Beam-Column Joints-

3.1 Introduction

In this study, reinforced concrete (RC) structural members with high strength concrete and reinforcement were analyzed using nonlinear finite element (FEM) in "FEM WG": Working Group of Constitutive Equations and Finite Element Method (FEM) (Chairman: Prof. H. Noguchi, Chiba University), in Sub-Committee on High-Strength Reinforcement (Chairman: Prof. S. Morita, Kyoto University) in New RC Project entitled "Development of Advanced Reinforced Concrete Buildings Using High-Strength Concrete and Reinforcement (Chairman: Emeritus Prof. H. Aoyama, the University of Tokyo), started in 1988. Most of the object specimens in the analysis were tested in Sub-committee on Structural Performances (Chairman: Prof. S. Otani, the University of Tokyo) in New RC project.

The constitutive models for FEM analysis of high strength RC structures were derived from the systematic basic experiment which was carried out in the "FEM WG". In the analysis, the emphasis of the investigation was laid on the shear behavior of RC members with high strength materials in order to make good use of the merit of FEM. The shear performance of RC members with high strength materials was also compared with that of RC members with ordinary strength materials. The five kinds of RC members: panels, shear walls, beams, columns, and beam-column joints, were analyzed in order to verify the applicability of FEM programs on the structural members of buildings.

Main items of the investigation in this study were as follows:

1. Modeling of nonlinear constitutive rules of high strength materials and its implementation to several FEM codes, including a platform program. The FEM analytical program, "FIERCM", which was developed by Prof. M. P. Collins, Dr. N. J. Stevens and Prof. S. M. Uzumeri in the Univ. of Toronto [3-1], was modified for high strength materials and used as a platform program. The original FEM codes developed in several universities, institutes and construction corporations were used for the comparisons and verifications.
2. RC members with high strength and ordinary strength materials were analyzed using several FEM codes as shown on Table 3-1 and the reliability of the program codes were investigated from the comparative analyses
3. The shear strength and deformation of RC members with high strength materials were investigated by FEM parametric analyses using several programs including a platform program.
4. Application of FEM analysis on the structural design of New RC building structures. (Analysis of a large-scaled box column of a New RC boiler building in a steam power plant using high strength materials.)

5. Guideline for the nonlinear FEM analysis of RC members with high strength materials. This guideline especially gives the know how and instructions for the nonlinear FEM analysis of RC members with high strength materials for design engineers and experimental researchers.

In this paper, the outline of the research results performed by the "FEM WG" was introduced by putting the emphasis on the above mentioned items No. 2 and No. 3.

3.2 Analytical Models for High-Strength Materials

3.2.1 Concrete

3.2.1.1 Stress-Strain Curves of Concrete

As for the main characteristics of the high strength concrete, the compressive stress-strain curve is nearly straight at the upward portion and the strength decay after the peak is remarkable as shown in Fig. 3- 1. The equation proposed by Fafitis and Shah [3-2] is commonly used for the high strength concrete.

The uniaxial compressive strength obtained form the test of cylinders is used for the analysis. The splitting strength obtained form the test of cylinders is used in the analysis of beams, columns and beam-column joints, but a square root of the compressive strength (unit: kgf/cm^2) is used in the analysis of panels and shear walls. Because the splitting strength is too large for panels and shear walls as compared with the previous test results.

The failure criteria on the bi-axial or tri-axial principal stress planes should be considered adequately as shown in Fig. 3- 2. The modeling of the confinement effects by lateral reinforcement is important especially for the analysis of beams, columns and beam-column joints.

The models proposed by Kent-Park [3-3][3-4] and Sakino in New RC WG for Confined Concrete are used in this study. While these models were proposed for the flexure problems, the models are also used in the analysis of flexural shear problems for convenience' sake. In high strength concrete, the confinement effects are not remarkable unless high strength reinforcement is used for the lateral reinforcement.

3.2.1.2 Tension-Stiffening Characteristics

Tension-stiffening model is commonly used for in the analysis for the representation of bond in the concrete between neighboring cracks. It was observed that the stress-decay after cracking was remarkable in high strength concrete and also in the specimens with large amount of reinforcement in the previous RC panel test performed by K. Sumi, Hazama-gumi Corp. in New RC FEM WG.

3.2.1.3 Compressive Strength Reduction Factor

It was pointed out that the strength and stiffness parallel to cracks of RC panels under tension and compression are lower than those of uncracked concrete under uniaxial compression in the previous panel test [3-5]. Therefore, in the analysis, the reduction factor was multiplied on the uniaxial compressive strength. It was pointed out that the reduction factor for the compressive strength of high strength concrete is smaller than that of ordinary strength concrete from the panel test. The reduction factors used for this study are shown in Fig. 3- 3. These factors were derived from the previous basic test performed by K. Sumi, Hazama-gumi Corp. in New RC FEM WG.

3.2.1.4 Shear Stiffness Reduction Factor

The shear stiffness reduction factor is used for the representation of shear transfer across a crack. This factor is considered to decrease according to the crack width like Al-Mahadi's model [3-6]. The shear stiffness reduction factor of high-strength concrete is also considered to decrease because of a crack passing though aggregates As there is not much data on the reduction factor on high strength concrete, the factor in accordance with the ordinary-strength concrete is used.

3.2.2 Reinforcement

The multi-linear or bi-linear model is used for the stress-strain curve of reinforcement. It should be noted that as for high strength reinforcement, the length of yielding plateau is shorter and the yielding ratio (yielding strength/tensile strength) is larger than those in ordinary strength reinforcement.

3.2.3 Bond

The bond stress-slip relationships are necessary for bond-link elements, but it is not easy to decide the relationships because of the effects of cover thickness, concrete strength, a position from a crack and so on. The relationships are decided in reference to the previous proposals [3-7] and the experiences of the analysis.

There is a tendency that the bond strength and stiffness of high strength concrete is proportional to σ_B or $\sigma_B^{2/3}$ (σ_B: compressive strength) as compared to those of ordinary strength concrete.

The research results obtained in the Working Group "Bond and Anchorage" (Chairman: Prof R. Tanaka, Tohoku Univ of Technology) in Sub-Committee on high strength reinforcement in the New RC project are useful and discussed in this study.

3.3 Comparable FEM Analyses of RC Members with High Strength Materials

3.3.1 Beams, Panels and Shear Walls

Comparable FEM analyses of RC beams, panels and shear walls were carried out using several FEM computer codes including a platform program, "FIERCM" (Stevens) [3-1] in order to verify the constitutive rules for RC with high strength materials.

The total number of analyzed specimens were 48.

1) Beams: 20 specimens
   - Ordinary strength: 4 specimens, selected specimens by JCI Committee on Shear Strength of RC Structures [3-8]
   - High Strength: 16 specimens
     New RC (PB, B series) tested by Prof. F. Watanabe, Kyoto Univ.
     ASB Series tested by Prof. H. Noguchi, Chiba Univ.
2) Panels: 12 specimens
   - High strength: New RC (Panel series) tested by Mr. K. Sumi, Hazama-gumi Corporation
3) Shear Walls: 16 specimens
   - Ordinary strength: 2 specimens, JCI selected specimens
   - High strength: New RC (NW series) tested by Prof T. Kabeyasawa, Yokohama National Univ.
     New RC (No 1 - No. 8) tested by Prof. Y. Kanoh, Meiji Univ. and Japan National Land Development Corporation

The FEM analyses were carried out by the following seven universities, institute and corporations.

a) Chiba University, Prof. H. Noguchi
b) Nihon University, Prof N. Shirai
c) Building Research Institute, Dr H. Shiohara
d) Ohbayashi-Gumi Ltd., Mr K Naganuma
e) Hazama-gumi Corporation, Mr. K Sumi
f) Fujita Corporation, Mr. K Uchida
g) Meiji University, Mr H. Takagi

As each example of the comparable FEM analyses, finite element idealization, analytical and experimental results and crack patterns are shown in Figs. 4 to 6 for a beam, a panel and a shear wall, respectively. The detailed investigation of the comparable analytical results are omitted in this paper.

The main problems which were pointed out for the constitutive laws from the comparable analyses are as follows,

1. The confinement effects by high strength lateral and longitudinal reinforcement on the ultimate shear strength of beams with high strength concrete were more remarkable than those in beams with ordinary strength materials.
2. Shear transfer effects by dowel action of reinforcement across a crack were considered to be relatively large when longitudinal and lateral reinforcement ratio were high in beams.
3. The analytical results of panels and shear walls gave a good agreement with the test results. When the failure mode is reinforcement yielding type, the modeling of the stress-strain curves of reinforcement is important, and it is desirable that the analytical curve is resemble to that obtained from the material test. When the failure mode is concrete compressive failure type, the modeling of the compressive strength reduction factor is important. As for the reduction factor, the analytical results where the effects of concrete strength and tensile principal strain were considered, gave a better agreement than those where only the effect of tensile principal strain was considered. As the analytical compressive strength reduction factor was based on the panel test, it is considered that the reduction factor is larger in beams and columns, the thickness of which is relatively larger than that of panels.

3.3.2 Columns

3.3.2.1 Analysis of Columns -1

The six short columns ($b \times D$ = 20cm × 20cm, a/D = 1.0) of NSK series with high strength concrete, σ_B = 58MPa and high strength reinforcement, σ_y = 735MPa, tested by H. Noguchi in Chiba Univ. were analyzed by H. Noguchi and A. Nimura in Chiba Univ. using their original FEM code. The parameters in the test were loading method (reversed cyclic and monotonic), lateral reinforcement (p_w = 0.3, 0.6, 1.8%), axial stress ratio ($n = \sigma_0 / \sigma_B$ = 0, 0.3, 0.6). The failure mode in the test was shear compression failure. Finite element idealization of the specimen is shown in Fig. 3-7.

In order to investigate the confinement effect, specimen NSK-7 with high ratio of reinforcement, p_w = 1.8% was analyzed using a plain concrete model, Kent-Park model [3-3] and modified Kent-Park model [3-4], as shown in Fig. 3-8. The improvement of the strength decay after a peak is considered in Kent-Park model, and the increase of the strength and the improvement of the ductility are considered in the modified Kent-Park model. From Fig. 3-8, it is indicated that the analytical results by the Kent-Park and modified Kent-Park models gave a better agreement with the test results as compared with that by plain concrete model. It is considered that the confinement effects of lateral reinforcement on core concrete gave an increase of the shear strength of the column.

As shown in Fig. 3-9, the analytical results under monotonic loading gave a good agreement for the shear strength with the test results of specimen NSK-2 under monotonic loading in the test of specimen NSK-1. The shear strength under reversed cyclic loading was lower than that of NSK-2 under monotonic loading.

The analytical results for parameters of lateral reinforcement and axial stress ratio are shown in Figs. 10 and 11, respectively, as compared with the test results. The analytical results gave a similar tendency with the test results.

3.3.2.2 Analysis of Columns -2

JCI four selected specimens with ordinary strength materials and eight specimens tested by Prof. K. Minami in Fukuyama University in New RC project with high strength materials were analyzed by Dr. K. Naganuma, Ohbayashi-gumi Corp., using their original FEM code, "FINAL".

The analytical results of columns with ordinary strength materials gave a good agreement except bond splitting failure type specimen No. 3 and specimen No 4 with high ratio of lateral reinforcement. As shown in Fig. 3-12, the plane stress analytical results of specimen No 4 where the confinement effect is not considered gave a lower maximum strength than the test result. The previous three-dimensional analytical results by K. Naganuma et al. [3-9] gave a good agreement with the test result. This indicated that the confinement effect is necessary to be considered in the analysis of the columns with high-ratio of lateral reinforcement

The analytical results of New RC columns, with high-ratio of lateral reinforcement with ties and sub-ties, p_w=1.19%, gave lower strength and smaller deformation as compared with the test, as shown in Fig 3-13. This tendency is remarkable in the case of high-axial stress ratio, $n = \sigma_0 / \sigma_B = 0.3$. If the lateral reinforcement ratio is high, it is considered that the confinement effects increase. In this condition, three-dimensional FEM analysis or plane stress FEM analysis in which the confinement effects are considered is necessary.

3.3.3 Analysis of Interior Column-Beam Joints

Three joint shear failure type specimens, OKJ-1,3,6 and two bond deterioration type specimens, MKJ-1,3 were tested and analyzed by H Noguchi and T. Kashiwazaki in Chiba University, using their original FEM code. This test was supported in New RC Working Group, "Beam-Column Joints and Frames" (Chairman: Prof S. Nomura, Tokyo University of Science)

The main parameter was concrete compressive strength σB 55MPa, 71MPa, 109MPa for OKJ=1, 3, 6 and 86MPa, 100MPa for MKJ-1, 3, respectively The shear reinforcement ratio in the joint, pw, was 0.54% The dimension and finite element idealization are shown in Figs 14 and 15, respectively

The analytical results on the joints shear stress-concrete strength are shown in Fig 3- 16, as compared with the test results and previous other test data for from ordinary to high strength concrete.

The analytical maximum joint shear stresses of the joint shear failure type specimen, OKJ-1,

3, 6 located on the area of from $5 \times \sqrt{\sigma_B}$ to $6 \times \sqrt{\sigma_B}$ (Unit: kgf/cm^2) [$1.57 \times \sqrt{\sigma_B}$ to $1.88 \times \sqrt{\sigma_B}$ (Unit: MPa)], and they gave a good agreement with the test results.

The analytical story shear force-story displacement relationships of specimens OKJ-1, 3, 6 and MKJ-1, 3, shown in Fig. 3-17 gave good agreements with the test results for both joint failure type, OKJ series and bond deterioration type, MKJ series.

The analytical deformation and crack pattern of specimens, OKJ-1, MKJ-1 at the maximum strength is shown in Fig. 3-18, as compared with the crack pattern of the test results. In the analysis of specimen, OKJ-1, the joint shear compression failure occurred after the compression failure of a beam. This was corresponding to the test results. In the analysis of specimen, MKJ-1, beam flexural yielding occurred, and an opening of the crack of a beam at the face of a column became wide because of the increase of slip out of beam longitudinal reinforcement. In the test, the joint shear compression failure was observed under the large deformation, story rotation angle R_s = 1/33rad., after beam flexural yielding But in the analysis this was not observed.

The analytical principal stress distributions of specimens, OKJ-1, MKJ-1 at R_s = 1/200rad and R_s = 1/33rad. at the maximum strength are shown in Fig 3-19 Though the compressive principal stress flew widely in the joint like a fan for both specimens at R_s = 1/200rad., the width of the compressive strut in the joint decreased and the compressive stress concentrated along the diagonal line in the joint at R_s = 1/33rad. This phenomenon was remarkable in the specimen, MKJ-1, in which the bond deterioration after the beam flexural yielding was dominant.

3.4 FEM Parametric Analyses of RC Members with High-Strength Materials

3.4.1 Beams

3.4.1.1 Analysis of Test Specimens

The five RC beams, ASB-1 - 4, 6 ($B \times D$ = 20cm × 30cm, a/D = 2.33) with high-strength materials tested by H. Noguchi and A. Amemiya in Chiba University were analyzed by H. Noguchi and N. Kobayashi, including parametric analyses using their original FEM code

The shear reinforcement ratios of the parameter were designed according to AIJ Guideline [3-10] using a concrete strength reduction factor in the draft of CEB Model code 1990, as shown in Fig. 3-20. The finite element idealization is shown in Fig 3-21. The symmetrical condition around a center point was used. The analytical shear force-story displacement relationships gave a good agreement with the test results except the specimen ASB-3, as shown in Fig 3- 22.

The analytical ultimate shear strength and the amount of shear reinforcement relationships are shown in Fig. 3-23, where the comparisons with the test results and the calculated results by the "A method" of AIJ Guideline using AIJ equation for the compressive strength reduction factor:

$\nu \times \sigma_B = \sigma_B \times (0.7-\sigma_B/2000))$, σ_B: concrete strength (kgf/m^2).

The analytical and calculated results gave a slightly conservative results. But it should be noted that the yielding of shear reinforcement and the compressive failure of the strut concrete were assumed in the "A method", but the yielding of the shear reinforcement was slightly observed in the FEM analysis.

3.4.1.2 FEM Parametric Analyses of Beams for the Amount of Shear Reinforcement

1) The Effects of Shear Reinforcement Ratios

The analytical shear strength and shear reinforcement ratio relationships are shown in Fig. 3-24, compared with the calculated results by the "A method" of AIJ Guideline. Here, the amount of beam longitudinal reinforcement was assumed to be large in order to avoid the flexural yielding. When p_w = 0.6%, the yielding of the shear reinforcement was remarkable, and the concrete crushing was not observed. When p_w = 0.8%, 1.2%, the yielding of shear reinforcement was seldom observed and the concrete compressive failure at the edge was observed at p_w = 1.2%. When p_w = 1.8%, 2.4%, 3.0%, the yielding of shear reinforcement was not observed, and the compressive failure of concrete strut occurred.

2) The Effects of Concrete Confinement Models with a Constant Value of $p_w \times \sigma_{wy}$

The FEM parametric analysis were carried out setting the value of $p_w \times \sigma_{wy}$ as a constant value for the specimen ASB-2. The Sakino model proposed in New RC WG on Confined Concrete and the modified Kent-Park model [3-4] were used for the confinement effects on the stress-strain curves by shear reinforcement. The comparisons of the stress-strain curves by the two confinement models are shown in Fig. 3-25.

The stress-strain curves by the New RC Sakino model and the modified Kent-Park model are shown in Fig. 3-26. The analytical shear force-deformation curves are shown for both models in Fig. 3-27. The analytical results by the modified Kent-Park model gave a difference for the ultimate shear strength according to the shear reinforcement, but there are almost no differences for the ultimate shear strength by Sakino model.

3.4.2 Columns

The column specimens which were tested by H. Noguchi and already mentioned in 3.3.2.1 were analyzed by H. Noguchi and A. Nimura in Chiba University, using their original FEM code. The parameters were shear reinforcement ratio P_w = 0.3%, 0.6%, 1.2%, 1.8%, and axial stress ratio, $n = N / {}_cN_u$ = 0, 0.1, 0.2, 0.3, 0.4, 0.5, 0.6, 0.8, 1.0, where ${}_cN_u$ is axial strength considering longitudinal reinforcement.

The analytical shear strength-axial stress ratio relationships as a parameter of shear reinforcement ratio are shown in Fig. 3- 28, compared with the test results. From the analysis of RC columns with ordinary strength materials performed by A Zhang and H.Noguchi [3-11], it was reported that the increase of shear strength is dominant in the case of low shear reinforcement ratio according to the increase if the axial stress ratio as compared with high shear reinforcement ratio.

As for the high strength materials, there was so much tendency that the shear strength increased in the case of low shear reinforcement ratio, according to the increase of the axial stress ratio. In this case, the increase of the shear strength according to the increase of the shear reinforcement ratio was remarkable even for the high axial stress ratio. The analytical results gave reasonable agreements with the test results for this tendency. It is considered that this tendency is depend on the confinement effect of shear reinforcement on core concrete.

The analytical shear strength-shear reinforcement ratio relationships as a parameter of axial stress ratio are shown in Fig. 3-29. Though the increase of the shear strength according to shear reinforcement ratio becomes a little blunt in the case of high axial stress ratio, this tendency is not remarkable than reported in ordinary strength concrete

FEM parametric analysis of columns with high strength materials was also carried out by K. Naganuma in Ohbayashi-Gumi Ltd The basic column specimens were mentioned in 3.3.2.2. The parameters were shear reinforcement ratio and axial stress ratio, $N/BD\sigma_b$ The analytical shear strength-shear reinforcement ratio relationships are shown in Fig 3-30. From this figure, the increase of the shear strength is large as the axial stress ratio is small. When the axial stress ratio is larger than 0.45, the effect of the difference of shear reinforcement ratios on the shear strength is small. The analytical shear strength and axial ratio relationships are shown in Fig. 3- 31. It is shown in this figure that the increase of the shear strength is remarkable as the shear reinforcement ratio is small

In this analytical model, the confinement effects by shear reinforcement on core concrete are not considered. As mentioned in 3 3 2 2, this analysis gave a lower strength than that in the test results in the case of higher ratio of shear reinforcement, P_w = 1.19%, under high axial stress, n = 0.30.

The analytical shear strength-shear reinforcement ratio relationships and the analytical shear strength-axial stress ratio relationships are shown in Figs 32 and 33, respectively The calculated strength by "A method" and "B method" in AIJ Guideline and the modified Arakawa's equation [3-12] The modified Arakawa's equation gave a similar tendency for the increase of the shear strength depending on the axial stress ratio but the analytical strength was higher than that in the modified Arakawa's equation.

The analytical shear strength located between "A method" and "B method" in AIJ Guideline [3-10] based on the equation in the draft of CEB model code [3-13] for the axial stress ratio less

than n = 0.3. The analytical strength was nearly corresponding to "A method" for no axial stress, and it was also corresponding to "B method" for the axial stress ratio, n = 0.3. The analytical strength gave a higher results than "B method" for the axial stress ratio higher than n = 0.3

3.4.3 Beam-Column Joints

3.4.3.1 Effects of Joint Shear Reinforcement Ratios and Concrete Strength

The beam-column joints were parametrically analyzed for the shear reinforcement ratio, P_w = 0, 0.09, 0.18, 0 36, 0.54, 0.9, 1.2, 2.4%, and concrete strength, σ_B = 21, 36, 51, 65, 80, 100, 120MPa, by H. Noguchi and S Takezaki in Chiba University, using their original FEM code. The basic specimen, AT-4, was tested also by them, with concrete strength, σ_B = 80MPa, and the yielding strength of beam longitudinal reinforcement, $_s\sigma_y$ = 556MPa and the yielding strength of shear reinforcement in the joint, σ_{wy} = 804MPa.

The analytical story shear force-story displacement relationships for 4 specimens of AT series with two failure modes of joint failure and beam flexural yielding gave reasonable agreements with the test results.

1) Effects of Joint Shear Reinforcement Ratios

In the parametric analyses, the amount of longitudinal reinforcement was increased in order to obtain the joint shear strength preventing the beam flexural yielding. The analytical story shear force-story displacement relationships are shown in Fig. 3-34. As for the specimens with small amount of joint shear reinforcement, P_w = 0, 0.09, 0.18%, the maximum strength is smaller than the other specimen with larger than P_w = 0.18% The analytical joint shear strength-joint shear reinforcement ratio relationships are shown in Fig. 3-35 The joint shear strength increased from P_w = 0 to P_w = 0 36%, and nearly reached the top of strength at P_w = 0.54%. Even if P_w = 2.4%, the remarkable increase of the strength is not observed.

2) Effects of Concrete Strength

The analytical joint maximum shear stress-concrete strength relationships are shown in Fig 3-36, compared with the previous test results. The analytical joint maximum shear stress increase in proportion of $\sigma_B^{2/3}$ (σ_B concrete strength), and they are located just above the curve of $6 \times \sqrt{\sigma_B}$ (Unit: kgf/cm^2), ($1\ 88 \times \sqrt{\sigma_B}$ (Unit. MPa).

3 4 3 2 Effects of Column Shear Force, Bond in Beam Longitudinal Reinforcement and Beam and Column Longitudinal Reinforcement Ratios

The analysis of beam-column joints are possible for the impractical condition using FEM. The following items were investigated by Dr H. Shiohara in Building Research Institute, using FEM code, "FIERCM" developed by Dr. N J Stevens et al in the University of Toronto [3-8]

1) In the previous design philosophy of beam-column joints, it has been considered that the shear force of a beam-column joint at the joint failure, $Q_j = T + C - Q_c$ is assumed to be constant. The joint maximum strengths are compared by the analysis of specimens (Case 1 and Case 3 in Fig. 3-37) with only the difference of the distance between contra-flexural points of columns.

As a result of the analysis, the joint maximum shear strength was not constant but changed by the changes of column shear force, when the distance between the contra-flexural points of columns was changed. The summation of input moments from both side beams was constant. Therefore, the assumption that the joint shear force = $(T + C - Q_c)$ at the joint failure is constant is considered not to be adequate.

2) In order to investigate the effects of bond in beam longitudinal reinforcement through a joint on the joint shear strength, the comparisons are made between a no bond specimen and a sufficient bond specimen.

As a result shown in Fig. 3-37, in the case of no bond in beam longitudinal reinforcement through a joint, the maximum input moment from beams to the joint was about a half of that in the case of perfect bond in beam longitudinal reinforcement.

3) The effects of beam and column longitudinal reinforcement ratios, which have not been considered in the previous design, are investigated. As a result shown in Fig. 3-37, the maximum input moment and the joint shear strength increased a little as beam longitudinal reinforcement ratio increased. But the effects of column longitudinal reinforcement ratio was not observed.

3.4.4 Shear Walls

3 4 4 1 Analyses of New RC Shear Walls

Fourteen shear wall specimens with high strength materials were analyzed including parametric analyses by Prof N. Shirai, Nihon University using the modified "FIERCM." The FEM code, "FIERCM", which was originally developed by Dr. Stevens, Prof. Collins and Prof. Uzumeri in the University of Toronto [3-8], was modified by installing the constitutive equations for high strength materials developed in "FEM WG" The object specimens were composed of the following two series,

1) NW series: 6 specimens tested by Prof T Kabeyasawa, Yokohama National University
2) No series. 8 specimens tested by Prof Y Kanoh, Meiji University and Japan Land Development Corporation

The analytical shear strength of these fourteen specimens are compared with the test results as shown in Fig. 3-38. The errors in FEM prediction were less than 5% for NW series and less than 12% for No. series.

3.4.4.2 Parametric Analyses of Shear Walls

The parametric analyses of shear walls were carried out in order to complement the parameter zone where the test data were not available. The four parameters were changed as follows,

1) Concrete Strength: σ_B = 200 - 1000kgf/cm^2
2) Wall reinforcement ratio: p_w = 0.2 - 1.45%
3) Column longitudinal reinforcement ratio: p_s = 1.5 - 6.25% (omitted in this paper)
4) Shear span ratio: h_w / L = 0.875 - 2.063 where the basic specimen had the same dimension and properties as the New RC specimen, No. 3.

The calculated results by the previous macroscopic model: Shohara-Katoh model [3-14], experimental equation: Hirosawa's equation [3-15] modified from Arakawa's equation and design equation in AIJ Guideline are compared with the FEM parametric analytical results for the four parameters in Figs. 39 - 41.

1) Effects of Concrete Strength

As for the effects of concrete strength on the shear strength shown in Fig. 3-39, as the compressive strength reduction factor, ν, Nielsen's equation: $\nu = 0.7 - \sigma_B/2000$ (kgf/cm^2) was adopted in the current AIJ guideline equation-1 [3-10]. CEB draft equation: $\nu = 3.68 \times \sigma_B^{2/3} / \sigma_B$ (kgf/cm^2) was used for AIJ Guideline equation-2. Modified CEB draft equation by "FEM WG": $\nu = 3.68 \times \sigma_B^{2/3} / \sigma_B$ (kgf/cm^2)> 0.5 was used for AIJ Guideline equation-3. The AIJ Guideline equation-3 gave the best agreement for the effect of concrete strength. The current AIJ Guideline equation-1 gave the results apart from the test and FEM analytical results as the concrete strength increased. Therefore, it is pointed out that the Nielsen's equation gave an excessive prediction for the reduction of the compressive strength of cracked high strength concrete.

2) Effects of Wall Reinforcement Ratios

The effects of the amount of wall reinforcement, $P_w \times \sigma_y$ (σ_y: yielding strength of reinforcement) on the shear strength are shown in Fig. 3-40. The AIJ Guideline-3 gave the best agreement with the test and FEM analytical results. However, all of the design equations gave an excessive prediction of the effects of wall reinforcement depend on the increase of $P_w \times \sigma_y$. Though the angle of the truss mechanism is assumed as $\cot \phi = 1$, there may be rooms for further investigation for high strength concrete.

3) Effects of Shear Span Ratios

The effects of shear span ratio on the shear strength are shown in Fig. 3-41. AIJ Guidelines equation-3 and Hirosawa's equation gave relatively good agreements with the test and FEM analytical results.

3.4.5 Panels

The estimation of shear behavior of RC panels is very important for the investigation of the shear strength and deformation of shear walls. The effects of the parameters which were not investigated in New RC panel test were parametrically analyzed. The parameters were reinforcing details: the combination of p_t and σ_y, uni-axial compressive stress and bi-axial compressive stress. Concrete strength was σ_B = 70MPa, and the failure mode was shear compression failure of panel concrete.

The analytical shear stress-shear strain relationships are shown in Figs. 42 - 44 From Fig. 3-42 for the effects of the combination of p_t and σ_y from $p_t \times \sigma_y$ = 20MPa, it is indicated that the analytical stiffness after shear cracking and the maximum strength increased as the wall reinforcement ratio, pt increased, even if $p_t \times \sigma_y$ was constant From Figs 43 and 44, it was observed that the axial compressive stress gave contributions toward the increase of the shear cracking strength and the shear strength This contribution was more remarkable in the case of bi-axial compression than that in the case of uni-axial compression

3.5. Concluding Remarks

In this paper, the principal research fruits were introduced. As for the high strength materials of reinforced concrete, the modeling of the stress-strain relationships, tensile strength, the compressive strength reduction factors of cracked high strength concrete, tension stiffness, shear modulus reduction factors of cracked high strength concrete and bond characteristics were discussed and established from the basic tests performed in New RC project These analytical models were installed into several FEM codes including a platform program, "FIERCM "

The principal members of RC buildings. panels, shear walls. beams, columns and beam-column joints, were analyzed systematically by the Working Group members using the several FEM codes The analytical results gave generally reasonable agreements with the test results, but the following problems were pointed out

1) Evaluation of the Compressive Strength Reduction Factors of Cracked High Strength Concrete

The analytical results of panels and shear walls gave good agreement with the test results, but the analysis of beams and columns gave conservative results as compared with the test results This tendency was more remarkable for the specimens with high ratio of shear reinforcement As the reduction factor was based on the panel test, it is considered that the reduction factor is larger in beams and columns, the thickness of which is relatively larger than that of panels The further investigations of the reduction factor are needed.

2) Confinement Effects of Cracked High Strength Concrete

The analysis gave a conservative results for beams and columns with high ratio of shear reinforcement. In this case, the confinement effects for the shear strength should be considered. In this study, the confinement effects were considered as the estimation of the stress-strain curves for the convenience of the plane stress analysis using the confinement model originally proposed for flexural confinement problems. The further investigations are needed for this conventional approach. The three-dimensional approach will be necessary for the essential solution of the problems of confinement effects.

3) As for the tension stiffness models and shear stiffness reduction factors, the further investigations are needed for several effecting factors.

4) The general estimation of bond in RC members with high strength materials are needed considering several effecting factors.

From the systematic FEM parametric analyses, the effects of the following parameters on the shear strength were investigated, and the applicability of the design and experimental equation was verified

1) Beams: $p_w \times \sigma_y$
2) Columns: axial stress ratio and p_w
3) Beam-column joints: p_w, σ_B
4) Shear walls. σ_B, $p_w \times \sigma_y$, p_t, and shear span ratio
5) Panels: $p_w \times \sigma_y$, σ_0 (uni-axial and bi-axial stresses)

As the further research subjects, the investigations of the shear and bond resistance mechanisms of RC members are necessary in order to verify the concepts of the truss and arch mechanisms proposed in the previous macroscopic models and to propose the more rational macroscopic models and design equations for the shear strength and deformation of RC members with high strength materials.

Acknowledgements

The works reported in this paper were discussed and performed by New RC Working Group on Constitutive Equations and FEM chaired by H. Noguchi, Chiba University and Sub-Committee on High Strength Reinforcement (Chairman Prof S Morita, Kyoto University). The author deeply acknowledge to the members of the working group and the sub-committee The works reported were also sponsored by the Ministry of Construction of Japan as a part of National Research Project, New RC (Chairman Emeritus Prof H. Aoyama, the University of Tokyo) The author wishes to express his gratitude to Prof M. P Collins, Dr N J Stevens and Prof S. M. Uzumeri in the University of Toronto for the use of FEM code, "FIERCM" as a platform program in the analytical works by the FEM WG

References

[3-1] Stevens, N. J., Uzumeri, S. M. and Collins, M. P.,"Analytical Modelling of Reinforced Concrete Subjected to Monotonic and Reversed Loading," Pub. No 87-1, Dept. of Civil Engrg., Univ. of Toronto, Jan. 1987.

[3-2] Fafitis, H. and Shah, S. P.,"Lateral Reinforcement for High Strength Concrete Columns," ACI SP, No.SP-87, 1985, pp.213-232.

[3-3] Kent, D. C. and Park, R.,"Flexural Members with Confined Concrete," Proc., ASCE, Vol.97, No.ST7, July 1971, pp.1969-1990.

[3-4] Park, R., Priestley, M. J. N. and Gill, W. D.,"Ductility of Square Confined Concrete Columns," Proc. ASCE, Vol.108, No.ST4, April 1982, pp.929-950.

[3-5] Vecchio, F. J. and Collins, M. P.,"The Modified Compression-Field Theory for Reinforced Concrete Elements Subjected to Shear," ACI Journal, Vol.83, No 2, Nov. 1986, pp.219-231.

[3-6] Al-Mahaidi, R. S. H.,"Nonlinear Finite Element Analysis of Reinforced Concrete Deep Members," Report 79-1, Dept. of Struct. Engrg., Cornell University, Jan. 1979.

[3-7] Morita, S. and Fujii, S.,"Bond Models Used in Finite Element Analysis," Finite Element Analysis of RC Structures, ASCE, 1986, pp.348-363.

[3-8] JCI Committee on Shear Strength of RC Structures, Collected Experimental Data for Verification of Analytical Models, Proc. of JCI Colloquium on Shear Analysis of RC Structures, JCI-C6, Oct. 1983 (in Japanese).

[3-9] Naganuma K., et al.,"Three-Dimensional Nonlinear FEM Analysis of RC Columns Under High Axial Force and Horizontal Forces," Proc. of AIJ Annual Meeting, Aug. 1992, pp.1065-1068 (in Japanese).

[3-10] Architectural Institute of Japan, Design Guideline for Earthquake Resistant Reinforced Concrete Buildings Based on Ultimate Strength Concept, 1990, pps 340 (in Japanese)

[3-11] Noguchi, H and Zhang A.,"Analytical Study on the Effects of Axial Force on the Shear Strength of RC Columns," Proc. of the JCI, Vol.13, No.2, 1991, pp 381-384 (in Japanese).

[3-12] Architectural Institute of Japan, Strength Potential and Deformation Performances in Aseismic Design of Buildings, 1990 (in Japanese)

[3-13] COMITE EURO-INTERNATIONAL DU BETON,CEB-FIP MODEL CODE FOR CONCRETE STRUCTURES, 1988.

[3-14] Shohara, R , Shirai N and Noguchi, H., "Verification of Macroscopic Models for RC Walls," Proc of ASCE Structure Congress, Structural Design, Analysis and Testing, May 1989, pp.291-290

[3-15] Hirosawa, M., "Strength and Ductility of Reinforced Concrete Members," Research Report for Buildings, No 76, Japan Association for Building Research Promotion, March 1977 (in Japanese).

Table 3-1 Systematic Finite Element Analyses of Specimens Selected by JCI and Tested in New RC Project

	Beam	Panel	Wall	Beam-column Joint	Column
Noguchi	[Ihzuka] JCI ASB NRC	[Ihuzuka, Zhang, Stevens] JCI NRC	[Ihzuka] JCI NRC HiRC	[Ihuzuka, Zhang] NRC {Joint WG}	[Zhang] NRC HiRC
Shirai		[Stevens] Collins (PV, PB)	[Stevens] JCI NRC		
Shiohara	[Stevens] NRC (PB, B) JCI			[Stevens] NRC	[Stevens] JCI HiRC NRC
Naganuma	[FINAL, Stevens] JCI NRC (PB, B) ASB		[FINAL] JCI NRC		[FINAL] JCI NRC
Sumi		[Stevens] NRC			
Takagi Shiraishi Suzuki {Wall WG}			[Meiji Univ.] NRC		
Uchida	[Fujita] NRC (PB, B) ASB				

[Researcher's or program's name]
{Working Group in New RC Project}

JCI : Specimens selected by Japan Concrete Institute
NRC : Specimens tested in National Research Project (New RC)
ASB : Specimens tested by Chiba University
HiRC : Specimens tested by Chiba University and Kajima Corporation

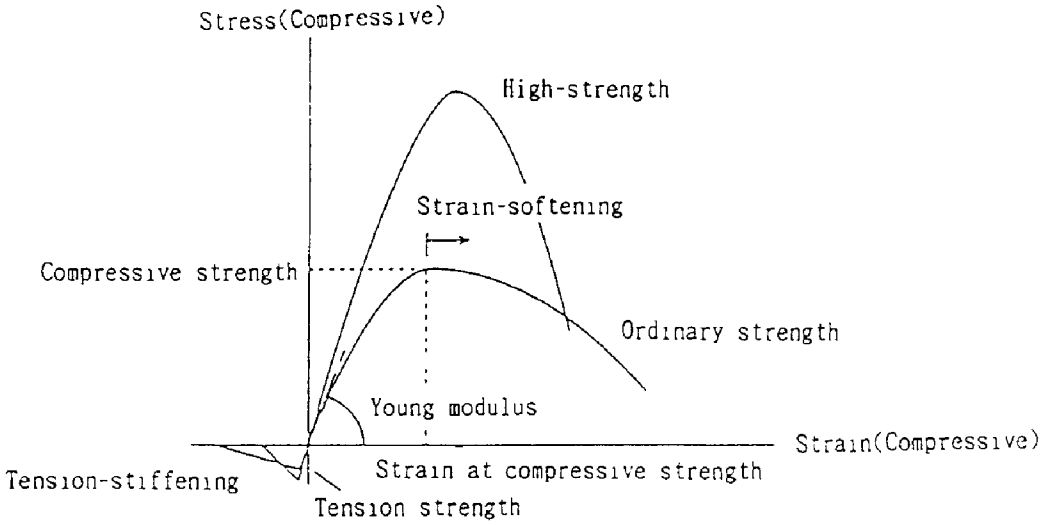

Fig. 3-1 Stress-strain Relationships of Concrete

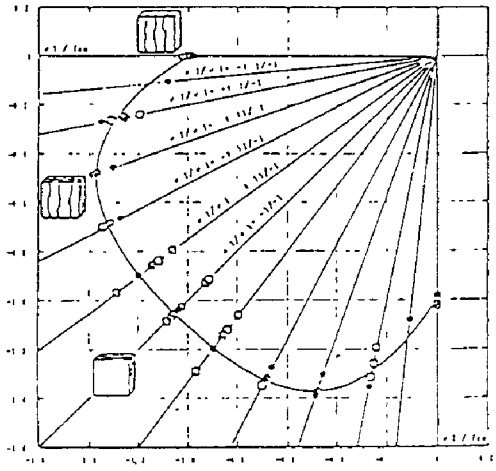

Fig. 3-2 Biaxial-criterion of High Strength Concrete

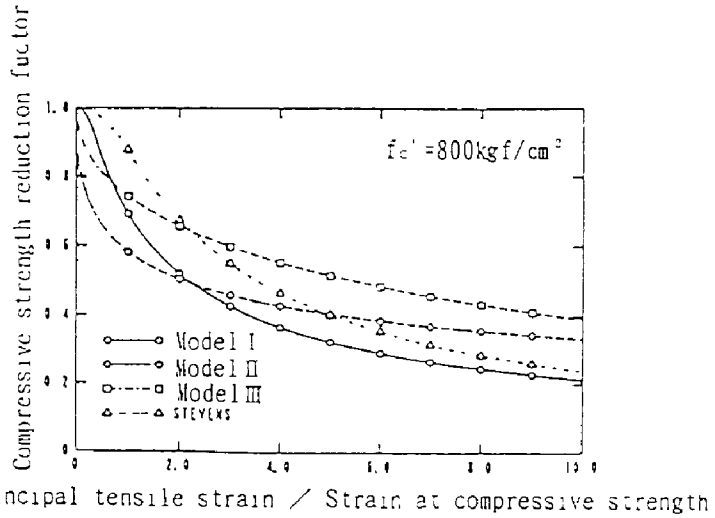

Fig. 3-3 Compressive Strength Reduction Factor for High Strength Concrete

Specimens for analysis

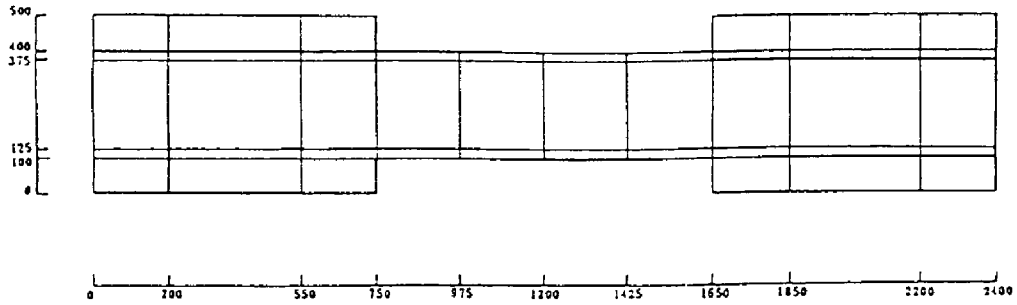

a) Finite Element Idealization

b) Comparisons of Analytical Results with Test Results of Beam PB4

	shear strength	Failure mode
Experimental result	74.5 tf	Flexural yielding
Shiohara's model	69.8 tf	–
Naganuma's model	66 8 tf	Flexural Compression failure
Uchida's model-1	43.6 tf	Shear compression failure
Uchida's model-2	61.9 tf	Shear compression failure(edge)

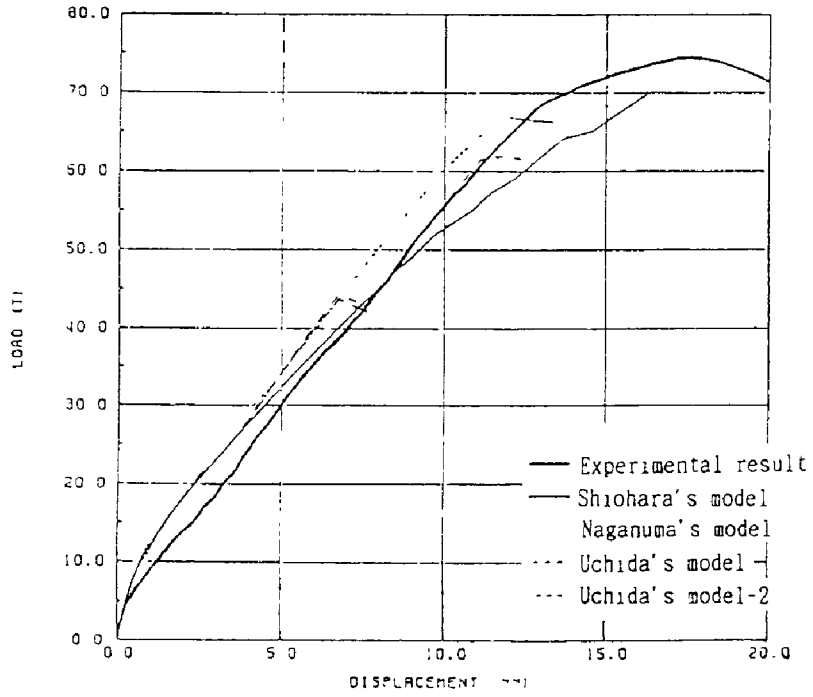

c) Load-Displacement Relationships

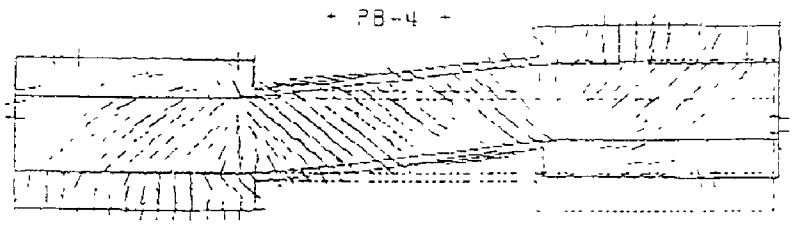

d) Crack Pattern (PB-4 at Maximum Strength)

Fig. 3-4 Finite Element Idealization and Analytical Results for New RC Beam PB4 Tested by Prof. F. Watanabe, Kyoto University

A panel is idealized as a single element.

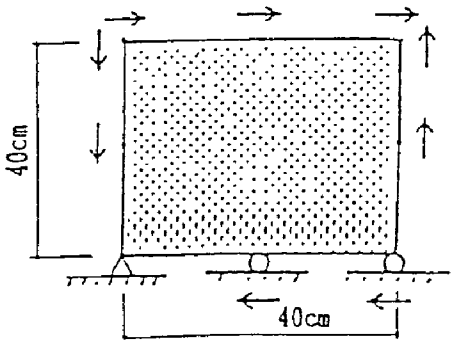

a) Finite Element Idealization

b) Comparisons of Analytical Results with Test Results of Panel 8-8-8

	shear strength	Failure mode
Experimental result	98.1 kgf/cm²	Cut off of reinforcement
Noguchi's model	95.5 kgf/cm²	Cut off of reinforcement
Shirai's model-1	104 3 kgf/cm²	–
Shirai's model-2	104.3 kgf/cm²	–
Shirai's model-3	103 8 kgf/cm²	–
Shirai s model-4	114 0 kgf/cm²	–
Shirai's model-5	104 3 kgf/cm²	–
Naganuma's model-1	112 0 kgf/cm²	Yielding of reinforcement
Sumi's model-1	106 5 kgf/cm²	Cut off of reinforcement
Sumi's model-2	105 8 kgf/cm²	Cut off of reinforcement
Takagi's model	92 0 kgf/cm²	–

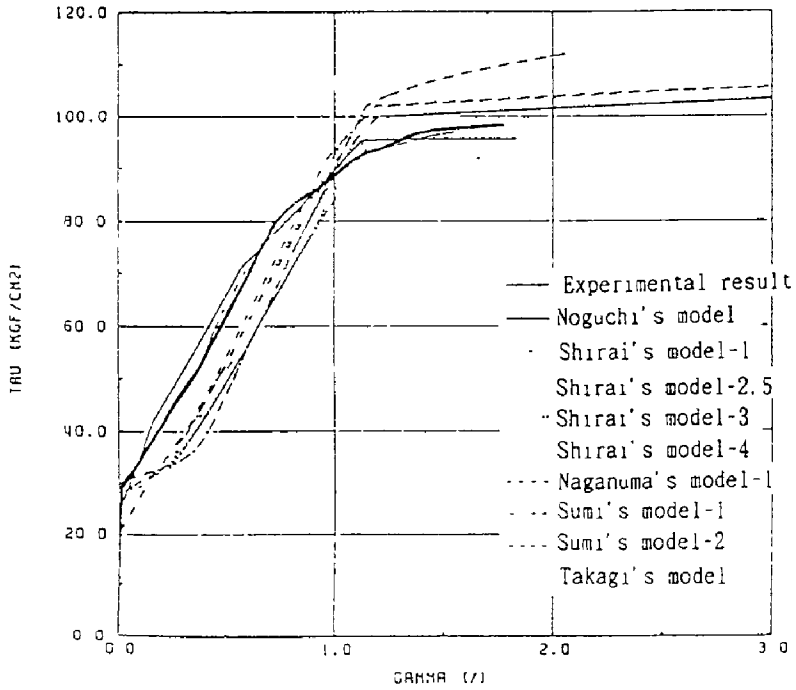

c) Load-Displacement Relationships

+8 −8−8+

Fig. 3-5 Finite Element Idealization and Analytical Results for New RC Panel Specimen, 8-8-8, Tested by K. Sumi of Hazama Corporation.

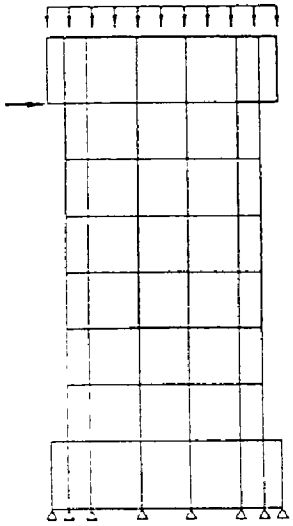

a) Shirai's Model

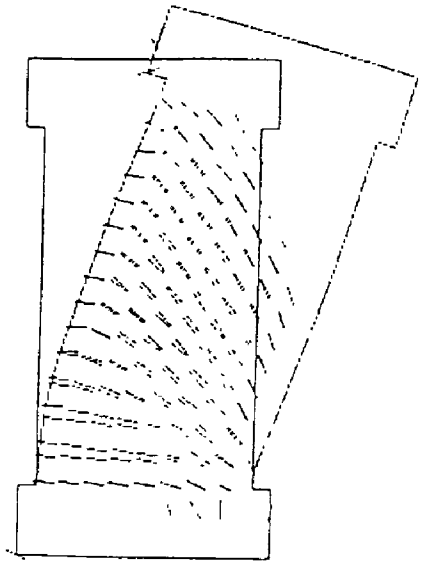

d) Crack Pattern (NW-1 at Maximum Strength)

b) Comparisons of Analytical Results with Test Results of Shear Wall NW-1

	shear strength	Failure mode
Experimental result	108 4 tf	Flexural failure
Noguchi s model	113 5 tf	Flexural yielding failure
Shirai's model-3	103.3 tf	–
Naganuma s model-1	103.6 tf	Compressive failure at the bottom of compression columns after flexural yielding
Takagi's model	101.9 tf	Compressive failure at shear wall after column flexural yealding

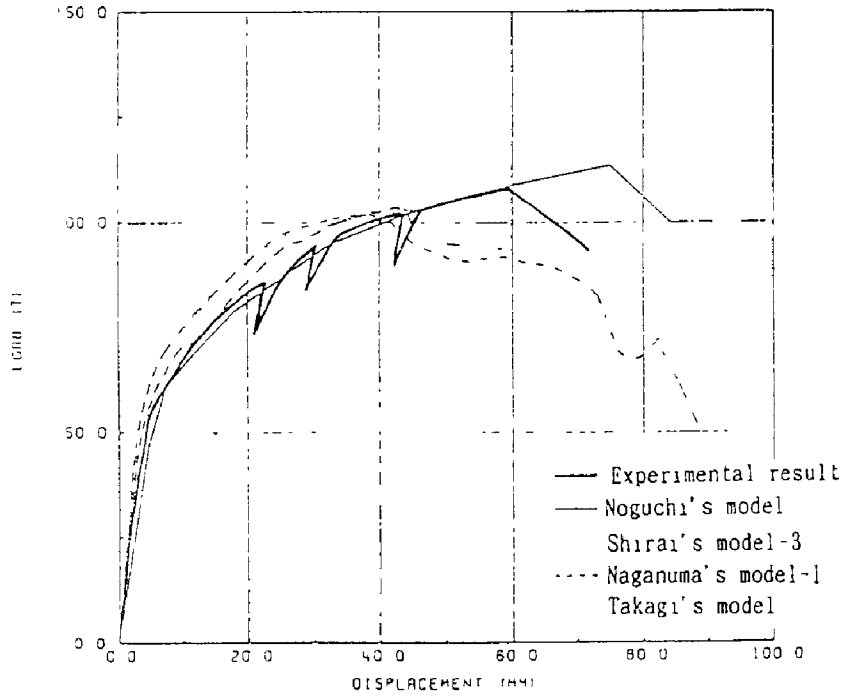

c) Load-Displacement Relationships

+ NW-1 +

Fig. 3-6 Finite Element Idealization and Analytical Results for New RC Shear Wall Specimen NW-1 Tested by T. Kabeyasawa of Yokohama National University

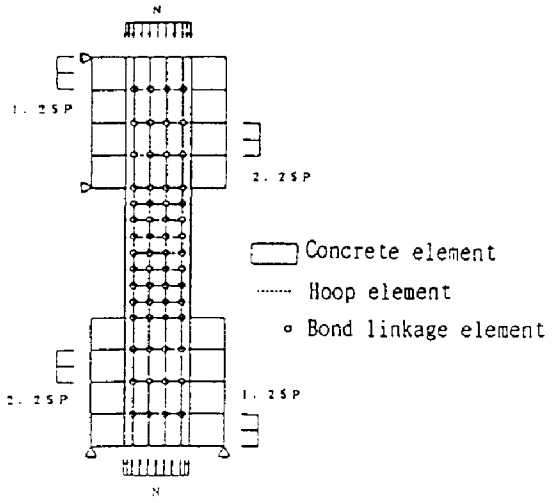

Fig. 3-7 Finite Element Idealization of Columns

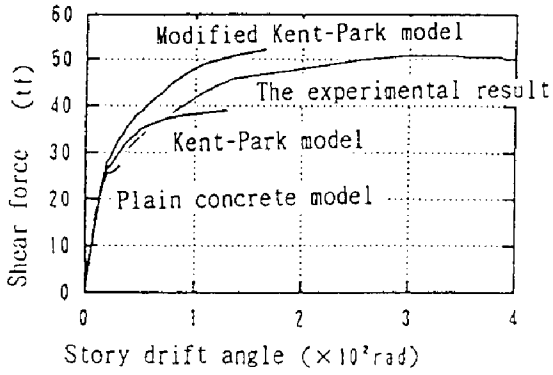

Fig. 3-8 Shear Force-Story Drift Angle Relationships (Influence of Confinement Effects(p_w=1.8%))

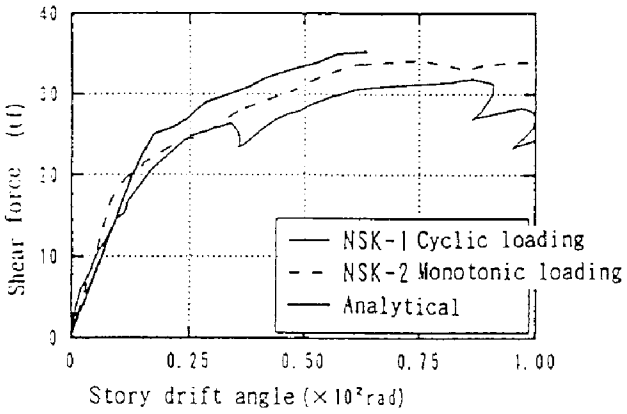

Fig. 3-9 Shear Force-Story Drift Angle Relationships (Loading Methods)

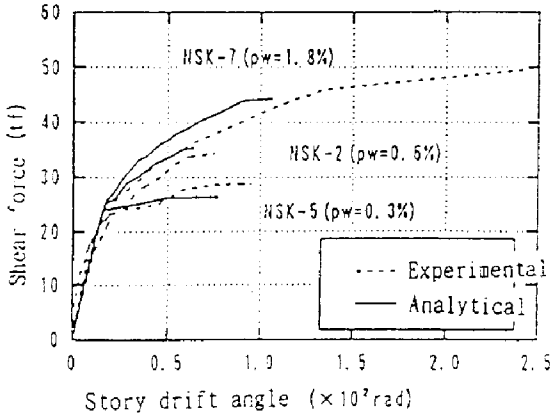

Fig. 3-10 Shear Force-Story Drift Angle Relationships (Lateral Reinforcement Ratio, p_w)

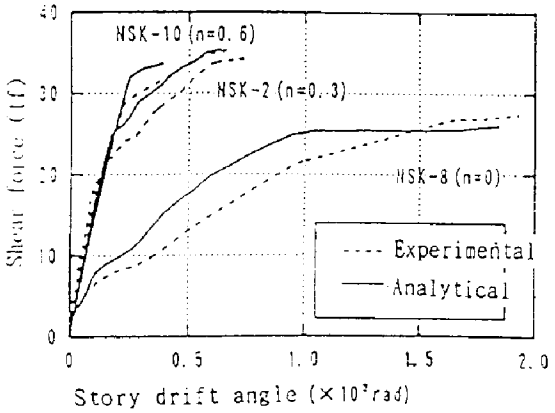

Fig. 3-11 Shear Force-Story Drift Angle Relationships (Axial Stress Ratio, n)

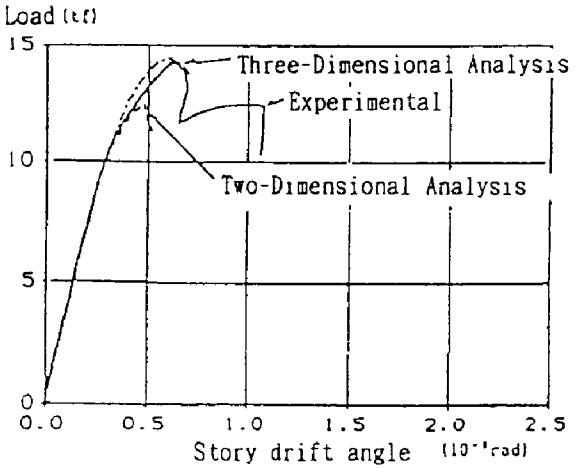

Fig. 3-12 Load-Story Drift Angle Relationships

JCI selected specimen No. 4

σ_B=241kgf/cm²
Main bar: 6-D10
Lateral reinforcement: 2-6ϕ

Axial stress ratio: n=0.581

σ_t=20.3kgf/cm²
p_g=0.68% σ_y=4458kgf/cm²
p_w=0.79%
σ_y=3804kgf/cm²

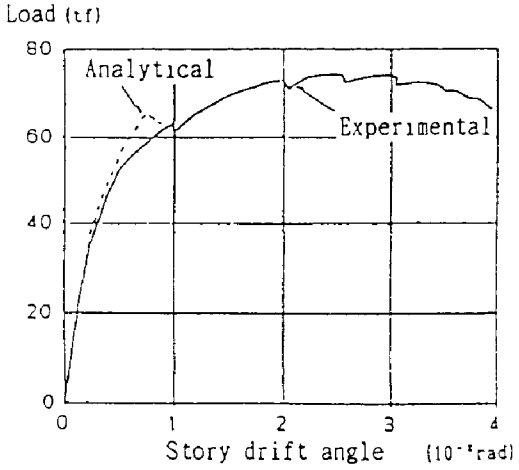

Fig. 3-13 Load-Story Angle Relationships

New RC selected specimen CA06-3-4

σ_B=735kgf/cm²
Main bar. 12-D19
Lateral reinforcement: 4-D10

Axial stress ratio: n=0.30

σ_t=49kgf/cm²
σ_y=7565kgf/cm²
p_w=1.19%
σ_y=10911kgf/cm²

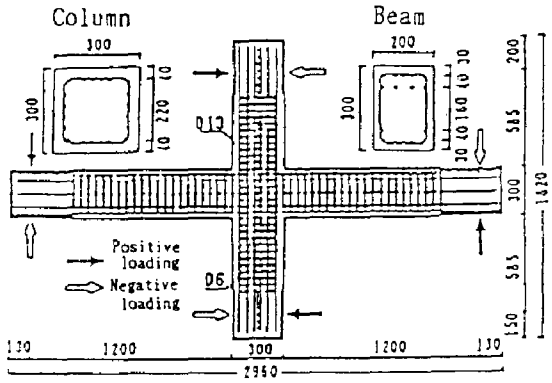

Fig. 3-14 Arrangement of Reinforcement (OKJ-1)

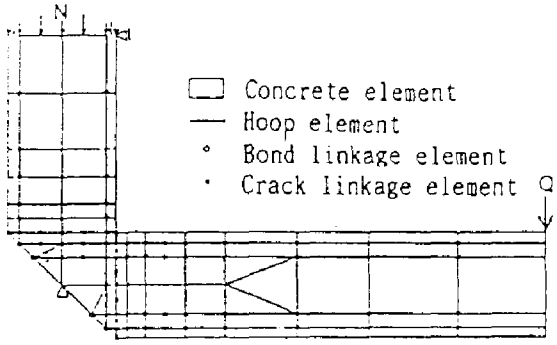

Fig. 3-15 Finite Element Idealization (OKJ)

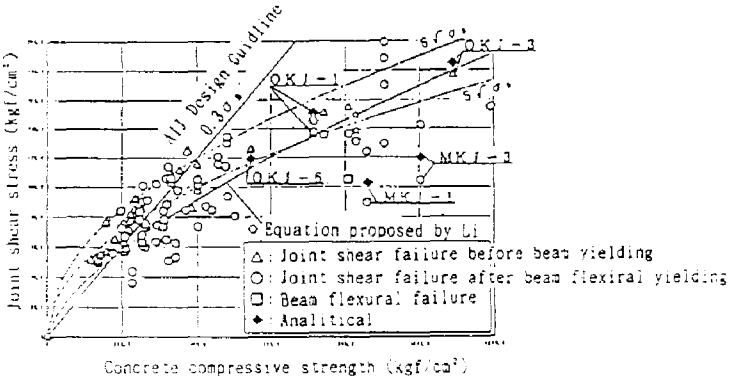

Fig. 3-16 Joint Maximum Shear Stress – Concrete Compressive Strength Relationships

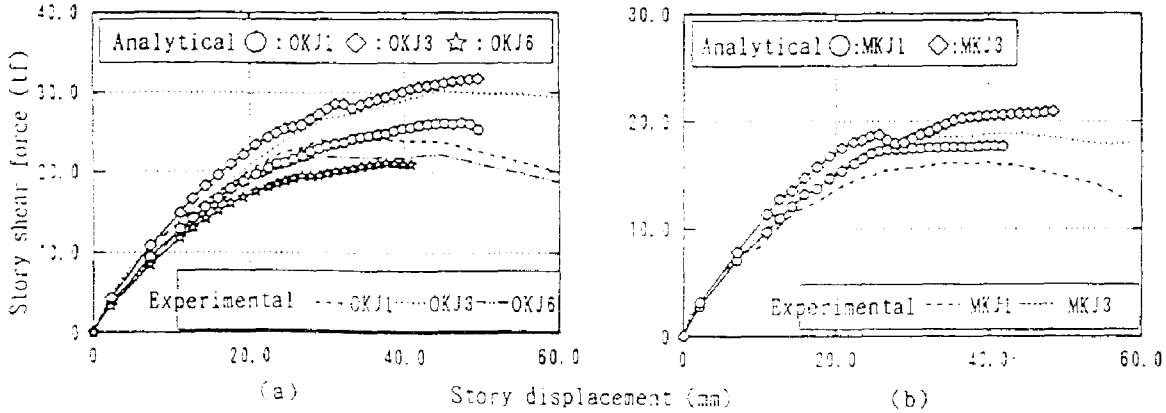

Fig. 3-17 Story Shear Force-Story Displacement Relationships

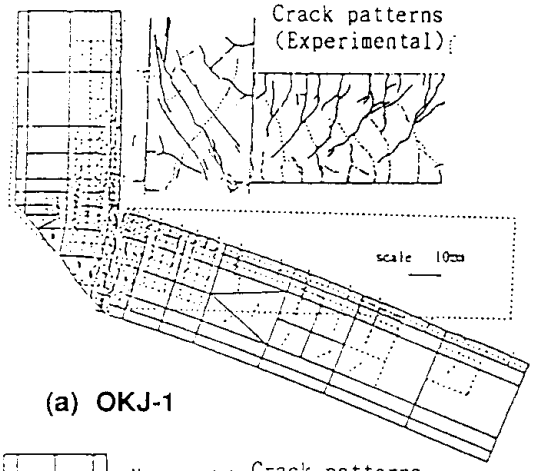

(a) OKJ-1

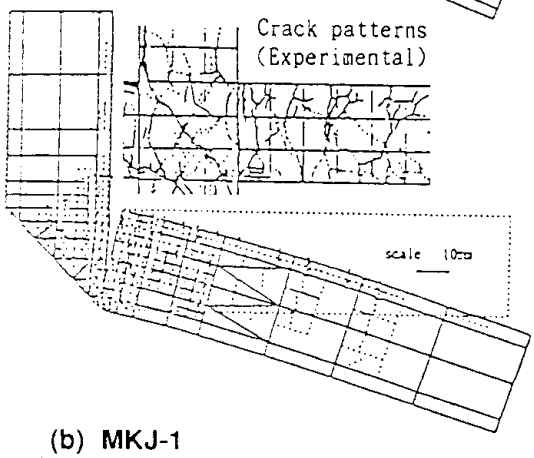

(b) MKJ-1

Fig. 3-18 Crack Patterns
(at maximum loading R_s=1/33rad.)

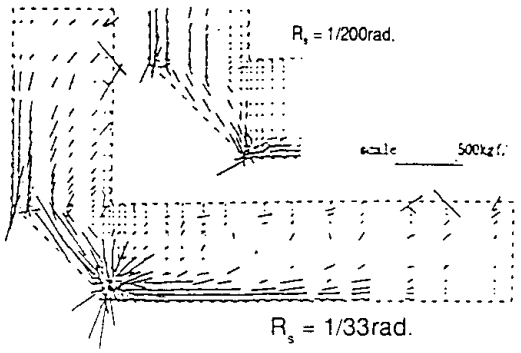

(a) OKJ-1

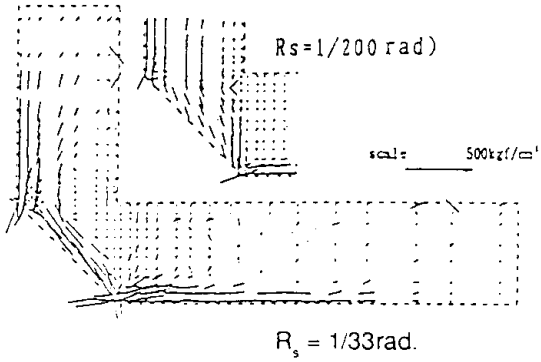

(b) MKJ-1

Fig. 3-19 Deformation Patterns
(at maximum loading R_s=1/33rad.)

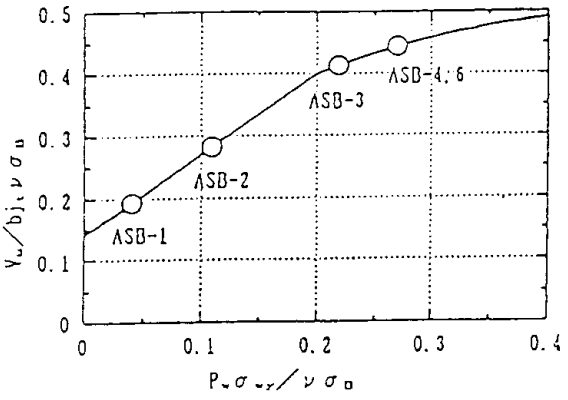

Fig. 3-20 Planning of Beam Test (Ultimate shear strength-amount of shear reinforcement relationships)

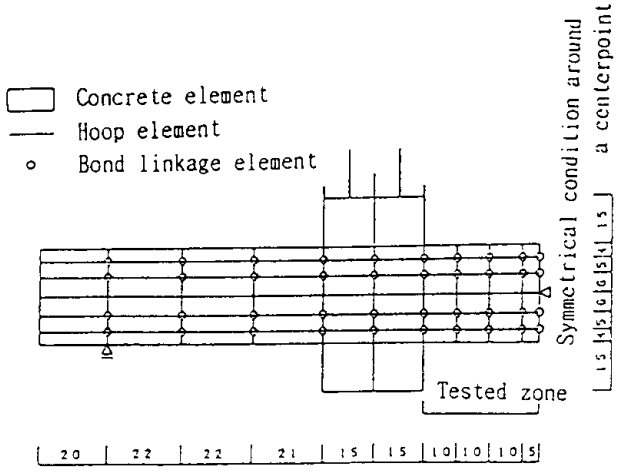

Fig. 3-21 Finite Element Idealization

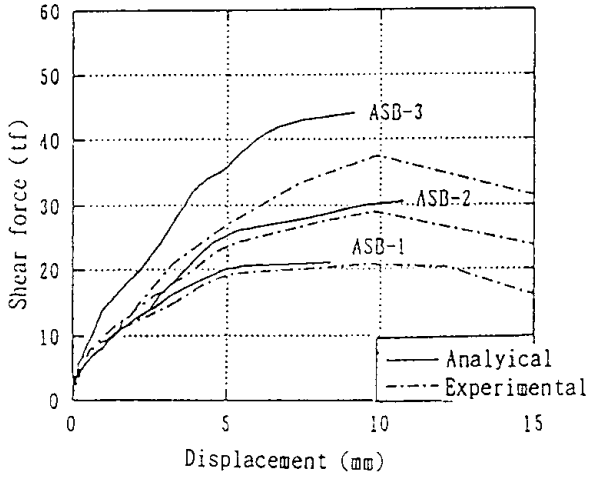

Fig. 3-22 (a) Shear Force-Displacement Relationships

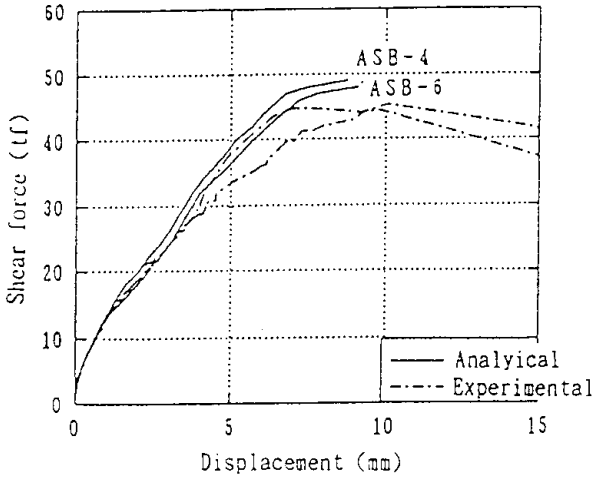

Fig. 3-22 (b) Shear Force-Displacement Relationships

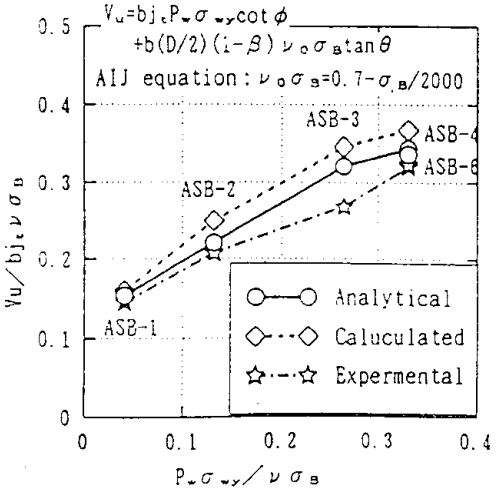

Fig. 3-23 Ultimate Shear Strength-Amount of Shear Reinforcement Relationships

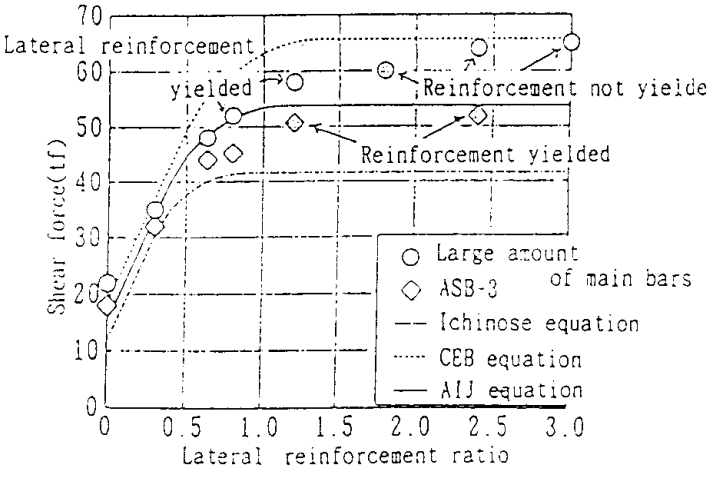

Fig, 3-24 Shear Force-Shear Reinforcement Ratio Relationships

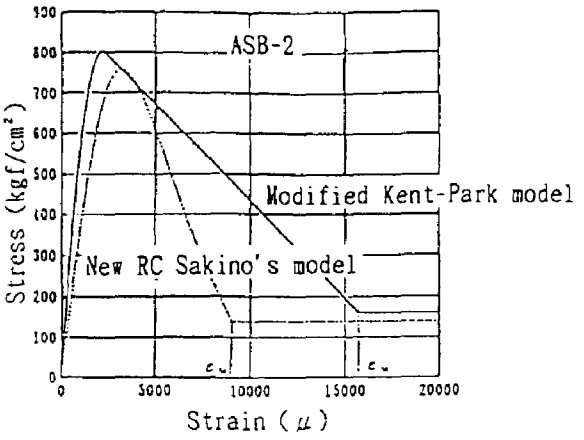

Fig. 3-25 Comparisons of the Stress-Strain Curves by the Two Confinement Models

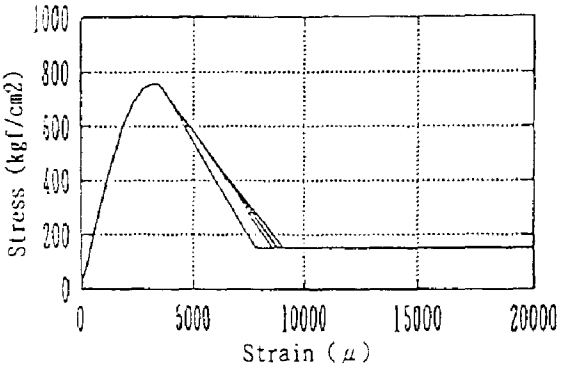

Fig. 3-26 (a) Stress-Strain Relationships Sakino's Model

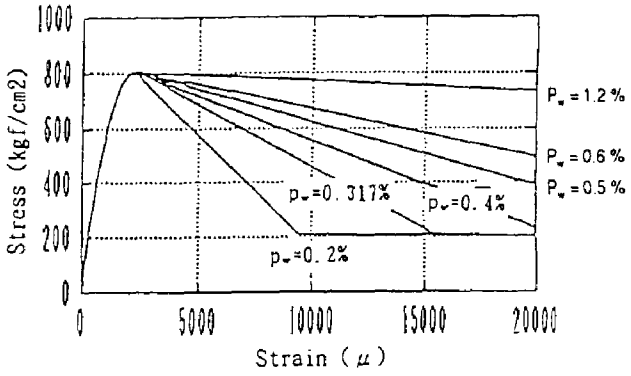

Fig. 3-26 (b) Stress-Strain Relationships Modified Kent-Park Model

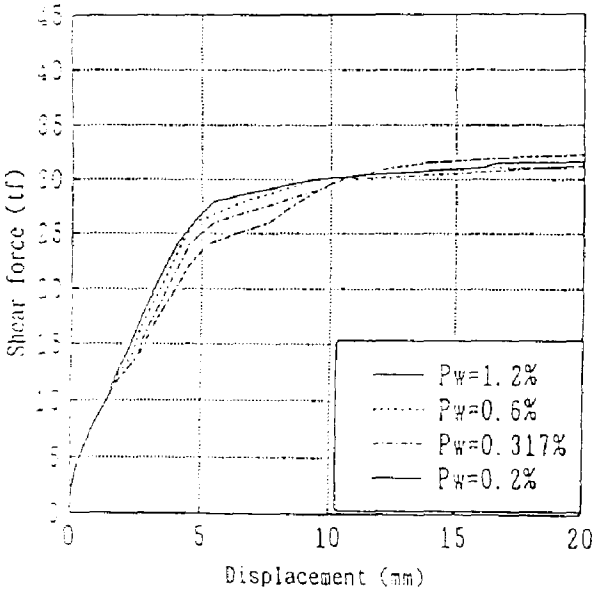

Fig. 3-27 (a) Shear Force-Displacement Relationships

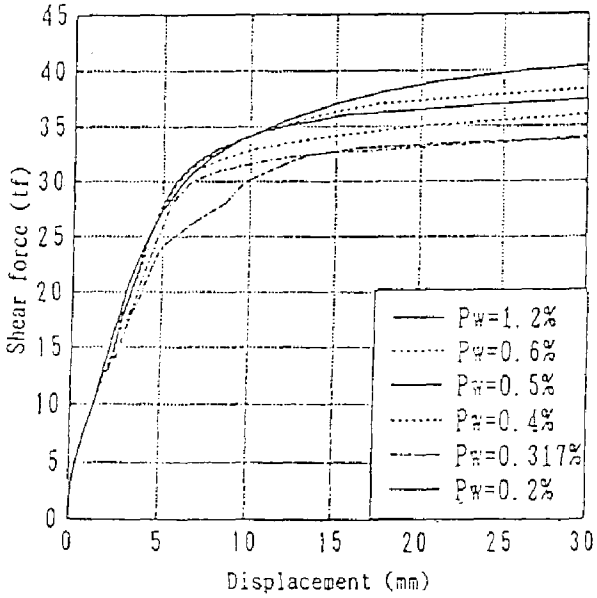

Fig. 3-27 (b) Shear Force-Displacement Relationships